Cancer Cell
Article

Bmi1 Controls Tumor Development in an Ink4a/Arf-Independent Manner in a Mouse Model for Glioma

Sophia W.M. Bruggeman,[1] Danielle Hulsman,[1] Ellen Tanger,[1] Tessa Buckle,[2] Marleen Blom,[1] John Zevenhoven,[1] Olaf van Tellingen,[2] and Maarten van Lohuizen[1,*]
[1]Division of Molecular Genetics
[2]Department of Clinical Chemistry
The Netherlands Cancer Institute, 1066CX, Amsterdam, the Netherlands
*Correspondence: m.v.lohuizen@nki.nl
DOI 10.1016/j.ccr.2007.08.032

SUMMARY

The Polycomb group and oncogene *Bmi1* is required for the proliferation of various differentiated cells and for the self-renewal of stem cells and leukemic cancer stem cells. Repression of the *Ink4a/Arf* locus is a well described mechanism through which *Bmi1* can exert its proliferative effects. However, we now demonstrate in an orthotopic transplantation model for glioma, a type of cancer harboring cancer stem cells, that *Bmi1* is also required for tumor development in an *Ink4a/Arf*-independent manner. Tumors derived from *Bmi1;Ink4a/Arf* doubly deficient astrocytes or neural stem cells have a later time of onset and different histological grading. Moreover, in the absence of *Ink4a/Arf*, *Bmi1*-deficient cells and tumors display changes in differentiation capacity.

INTRODUCTION

The Polycomb group (PcG) gene and epigenetic silencer *Bmi1* was originally identified as a collaborating oncogene in the induction of lymphoma (Haupt et al., 1991; van Lohuizen et al., 1991) and was subsequently reported overexpressed in various human cancers (Valk-Lingbeek et al., 2004). Its oncogenic function has mainly been contributed to its repressive effect on the *Ink4a/Arf* tumor suppressor locus (Jacobs et al., 1999). However, recent studies have demonstrated that PcG proteins bind to multiple regions of the genome and therefore should have several additional targets (Boyer et al., 2006; Bracken et al., 2006; Lee et al., 2006; Negre et al., 2006; Tolhuis et al., 2006). In line with this, we observed that while deletion of the *Ink4a/Arf* locus can rescue a number of *Bmi1* knockout phenotypes, other deficiencies in, for instance, the brain remain (Bruggeman et al., 2005). Therefore, we decided to test whether *Bmi1* is required in an *Ink4a/Arf*-independent manner for the formation of high-grade glioma, an incurable cancer of the brain.

Gliomas can be divided into WHO grade II–IV tumors (Kleihues et al., 2002). Grade II to III tumors consist of glial cells only and are classified as either astro-, oligo-, or mixed oligoastrocytomas. Grade IV tumors have a variable appearance and are sometimes referred to as glioblastoma multiforme (GBM). They contain necrotic areas surrounded by pseudopalisading tumor cells, regularly display hyperproliferation of the endothelium, and sometimes exhibit neuronal differentiation. GBM can develop de novo (primary GBM) or from a preexisting lower grade glioma (secondary GBM). Interestingly, it has been demonstrated that human GBM harbors "tumor-initiating cells" or "cancer stem cells" (CSCs) (Galli et al., 2004; Hemmati et al., 2003; Singh et al., 2004). CSCs represent a rare subpopulation of cells within the tumor bulk that

SIGNIFICANCE

The Polycomb group and oncogene *Bmi1* prevents premature growth arrest in most differentiated tissue cells and is essential for the self-renewal of several types of adult stem cells. Previous studies documented the *Ink4a/Arf* tumor suppressor locus as the main target mediating these activities. However, not all defects in the *Bmi1* knockout mouse can be contributed to *Ink4a/Arf* misregulation, suggesting additional factors to be involved. Our current report that *Bmi1* plays a role in pathways controlling proliferation, adhesion, and differentiation in mouse brain cancer in an *Ink4a/Arf*-deficient background highlights that *Bmi1* controls multiple processes in association with genes other than *Ink4a/Arf*.

has the unique capacity to give rise to new tumors upon transplantation. They have been identified in a number of solid cancers as well as leukemia (Al Hajj et al., 2003; Bonnet and Dick, 1997; Lapidot et al., 1994). CSCs share features with normal adult stem cells like the expression of primitive markers and capability to self-renew and differentiate. Consequently, genes controlling normal stem cells may also play a role in the cancer stem cell compartment. From this respect, it is particularly interesting that, in addition to a requirement for the proliferation of a variety of differentiated cells, *Bmi1* has been shown to be essential for the proliferation and self-renewal of several adult stem cells, among which are the neural stem cells (NSCs) of the subventricular zone (SVZ) (Bruggeman et al., 2005; Leung et al., 2004; Molofsky et al., 2003; Molofsky et al., 2005; Park et al., 2003; Zencak et al., 2005). Moreover, *Bmi1* is necessary for the propagation of leukemic stem cells and is expressed in glioma stem cells (Hemmati et al., 2003; Lessard and Sauvageau, 2003).

Recent advances in glioma modeling in the mouse have made the disease amenable to in vivo functional and molecular genetic studies (Fomchenko and Holland, 2006). Taking into account that the hypothesis that fully differentiated astrocytes act as cell of origin for glioma is currently challenged by studies demonstrating that NSCs or progenitors serve as source (Sanai et al., 2005; Zhu et al., 2005), we took advantage of an existing orthotopic transplantation model in which either primary NSCs or astrocytes are used as cell of origin for the disease (Bachoo et al., 2002). In this model, two mutations frequently found in GBM are employed: deficiency for *Ink4a/Arf* in combination with a constitutively active mutant EGF receptor (*EGFR) (Ekstrand et al., 1992; Nishikawa et al., 1994; Zhu and Parada, 2002). In tissue culture experiments, we observed that *Bmi1* absence in an *Ink4a/Arf*-deficient background inhibits *EGFR induced transformation and found this effect reflected in vivo. *Bmi1*-deficient tumors form with a later onset, have different histological grading, and exhibit reduced neuronal differentiation, suggesting that *Bmi1*, independently from repression of the *Ink4a/Arf* locus, regulates growth and fate of glioma tumor cells.

RESULTS

Bmi1 Is Required for In Vitro Transformation of *Ink4a/Arf*-Deficient Astrocytes

Before studying the role of *Bmi1* in the development of brain cancer from NSCs and astrocytes, we verified that *Bmi1* is expressed in these cells in vivo (Figure 1A; Figures S1A and S1B in the Supplemental Data available with this article online). We found that Bmi1 is present in most brain cells and that expression is particularly high in the SVZ, the major neurogenic region where the stem cells and progenitors reside. Identical results were obtained with *Ink4a/Arf*$^{-/-}$ mice (Figures S1C–S1E).

Next, we set out to assess whether absence of *Bmi1* has an effect on the proliferative capacity of cortical astrocytes. Hereto, we isolated primary cell cultures from cerebral cortices from 7-day-old mice according to established methods, taking care to avoid the SVZ region. These polyclonal cultures contained approximately 70% GFAP+ (glial fibrillary acidic protein, an astroglial marker) cells and were negative for Nestin or TuJ1 (progenitor and neuronal markers, respectively) (Figures S2A, S2C, and S2E). Since in vivo (though not in vitro) GFAP also labels SVZ stem cells (Doetsch et al., 1999; Garcia et al., 2004; Imura et al., 2003; Laywell et al., 2000; Figure S10D), we investigated the expression of another progenitor marker, the carbohydrate LeX/SSEA-1/CD15 (Imura et al., 2006). This marker is only rarely found on cells in our cultures and its expression is not significantly different between *Ink4a/Arf*$^{-/-}$ and *Bmi1*$^{-/-}$;*Ink4a/Arf*$^{-/-}$ cultures (Figures S2B and S2D). Hence, we will refer to these cultures as astrocytes, even if formally a minor contamination of more primitive cells cannot be ruled out.

In a 3T3 proliferation assay, *Bmi1*$^{-/-}$ astrocytes undergo premature growth arrest (Figure 1B). Codeletion of the *Ink4a/Arf* locus rescues this phenotype and immortalizes *Bmi1*$^{-/-}$ cells. However, derepression of the *Ink4a/Arf* locus is not causing all *Bmi1*$^{-/-}$ abnormalities (Figure S3) (Bruggeman et al., 2005). Therefore, we set out to find *Ink4a/Arf*-independent functions for *Bmi1* in a model system for in vitro transformation of *Ink4a/Arf*$^{-/-}$ astrocytes (Bachoo et al., 2002). In this model, primary *Ink4a/Arf*$^{-/-}$ astrocytes deprived from serum but stimulated with the growth factor EGF in defined NSC growth medium rapidly undergo morphological changes resembling loss-of-contact inhibition and acquisition of anchorage-independent growth, both hallmarks of transformation (Freedman and Shin, 1974; Wang, 2004). For simplicity, we will refer to this phenotype as EGF-induced transformation. First, we verified that this feature was due to *Ink4a/Arf* absence and not to contaminating progenitor cells. Hereto, we isolated astrocytes engineered with LoxP sites flanking the *Ink4a/Arf* locus. We only found clear morphological changes upon EGF stimulation when they were transduced with a Cre-recombinase, which causes the region between the LoxP sites to be acutely excised from the genome (Figure 1C). Remarkably, *Ink4a/Arf*$^{-/-}$ cells lacking *Bmi1* are completely incapable of adopting the transformed morphology, which demonstrates that *Bmi1* is involved in transformation in an *Ink4a/Arf*-independent manner (Figure 1D). Importantly, we could mimic this by removing *Bmi1* from *Ink4a/Arf*$^{-/-}$ cells using a short hairpin vector against Bmi1 (shBmi1) (Figure 1E). This shRNA had efficiently removed Bmi1 mRNA (Figure 1F) and protein (Figure 1G). Notably, we observed a minor induction of both Bmi1 mRNA (Figure 1H) and protein (Figure 1I) during the process of transformation.

Immunophenotypical analysis revealed that both control and *Bmi1*-deficient cells stimulated with EGF for 2 weeks were positive for GFAP, LeX, and Nestin (Figure 2A). If they were subsequently treated with 2% serum (FBS) for 5 days, control cultures partially switched off the stem/progenitor markers and started to generate TuJ1+ neurons (Figure 2B). However, the *Bmi1*$^{-/-}$;*Ink4a/Arf*$^{-/-}$

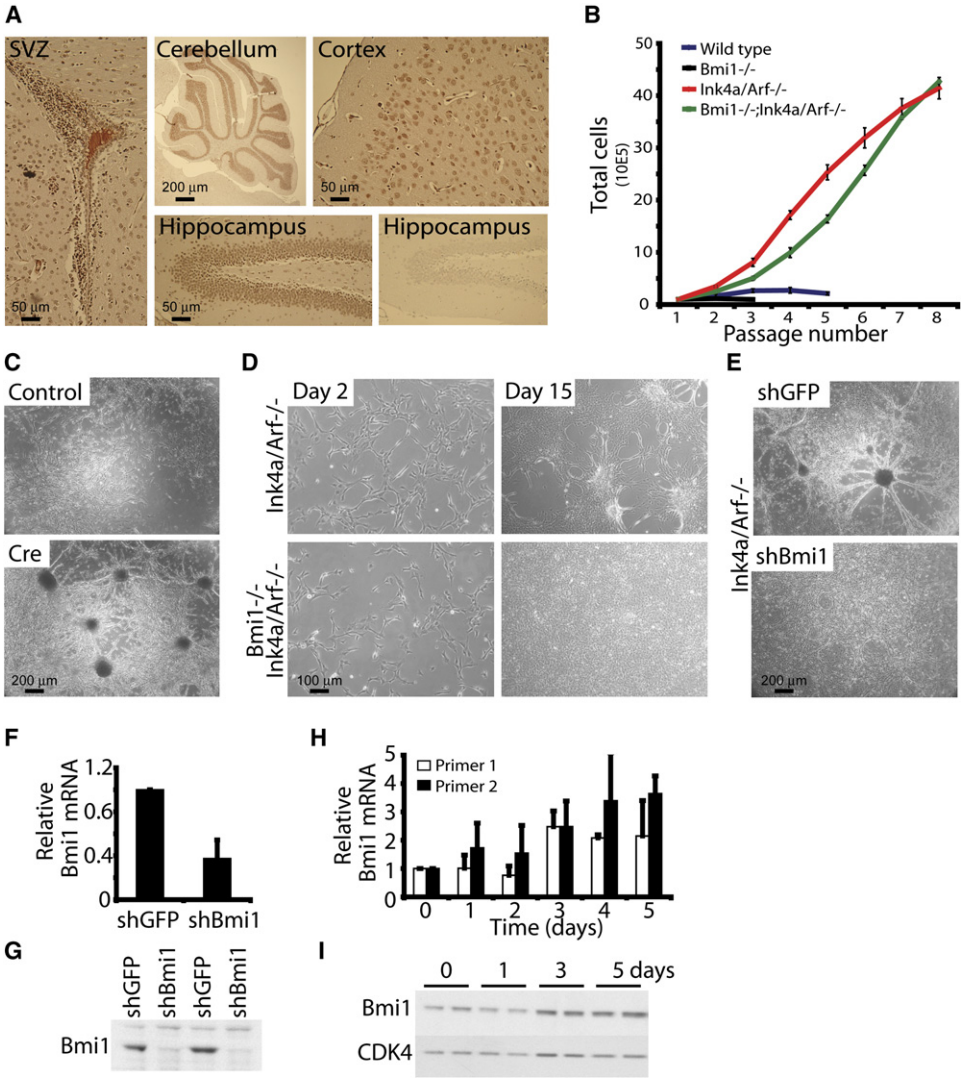

Figure 1. *Bmi1* Is Required for Transformation of *Ink4a/Arf*$^{-/-}$ Primary Astrocytes

(A) Immunohistochemical staining for Bmi1 protein in neurons of the cerebellum, cortex, and hippocampus (middle and right top panels, middle bottom panel), and astrocytes of the corpus callosum (left panel). Particularly high Bmi1 expression in the SVZ (left panel). No Bmi1 was detected in the *Bmi1*$^{-/-}$ hippocampus (right bottom panel).

(B) 3T3 proliferation assay of primary astrocyte cultures. Cells were passaged every 3 days.

(C) Astrocytes engineered with LoxP sites flanking the *Ink4a/Arf* locus are transduced with Cre-recombinase or control retrovirus. They were subjected to EGF stimulation and serum withdrawal for 14 days and scored for morphological changes.

(D) *(Bmi1*$^{-/-}$*;)Ink4a/Arf*$^{-/-}$ astrocyte cultures were stimulated with EGF for 2 days (left panels) or 15 days (right panels) in the absence of serum. Note marked differences in transformed morphology.

(E) *Ink4a/Arf*$^{-/-}$ astrocytes were transduced with retrovirus expressing an shRNA against Bmi1 (shBmi1) or a control shRNA against GFP (shGFP) and subsequently stimulated with EGF for 14 days in the absence of serum.

(F and G) Reduced Bmi1 mRNA (F) and protein (G) levels in astrocytes transduced with shBmi1 as demonstrated by qRT-PCR and western blot analysis, respectively.

(H) Induced Bmi1 mRNA and (I) protein levels upon stimulation of *Ink4a/Arf*$^{-/-}$ astrocytes with EGF in the absence of serum in time.

Error bars represent the average of two independent experiments ± SD (B, F, and H)

populations hardly ever contained neurons. To test if rare LeX+ cells were responsible for these phenotypes, we sorted both *Ink4a/Arf*$^{-/-}$ and *Bmi1*$^{-/-}$*;Ink4a/Arf*$^{-/-}$ astrocyte cultures into LeX positive and negative fractions (Figure S4A), stimulated these cells for 2 weeks with EGF, and subsequently induced differentiation for 5 days with 2% FBS (Figure S4B). We found no differences between the positive and negative fractions, neither in transforming capacity nor in marker expression, suggesting that LeX+ cells are not exclusively capable of undergoing EGF-induced transformation or generating neurons. Importantly, LeX+ *Bmi1*-deficient fractions were no more

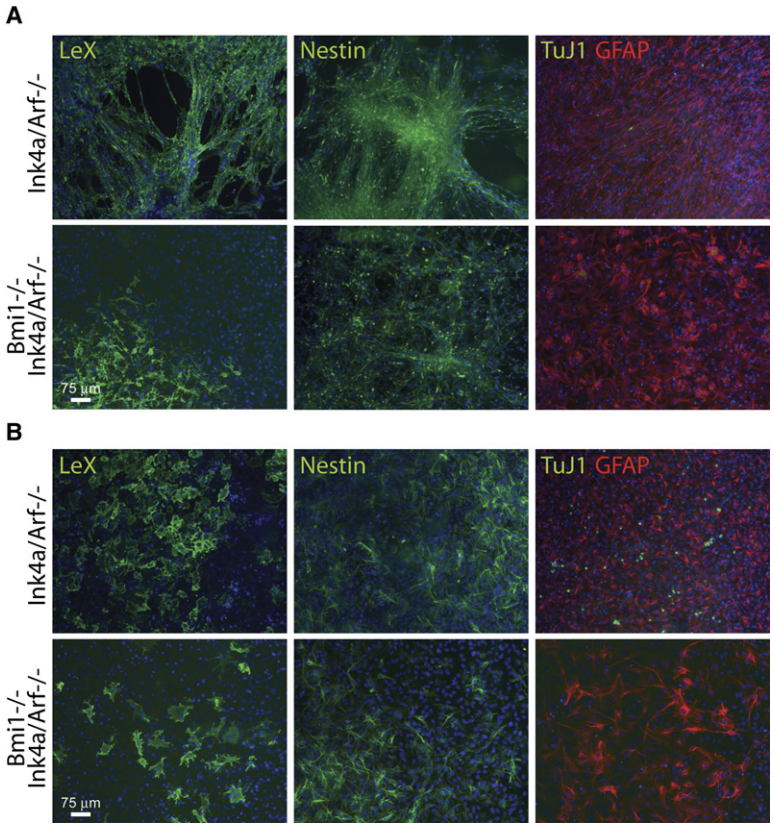

Figure 2. Immunophenotypical Characterization of EGF Stimulated Astrocytes

(A) *(Bmi1*$^{-/-}$*;)Ink4a/Arf*$^{-/-}$ astrocyte cultures were stimulated with EGF for 14 days in the absence of serum. They were stained for LeX/SSEA-1/CD15 (green, left panels), Nestin (green, middle panels) or TuJ1 (green, right panels) and GFAP (red, right panels). Nuclei were counterstained with DAPI (blue).

(B) Following 14 days of EGF stimulation, *(Bmi1*$^{-/-}$*;)Ink4a/Arf*$^{-/-}$ astrocyte cultures were treated with 2% serum (FBS) for 5 days. They were stained for LeX/SSEA-1/CD15 (green, left panels), Nestin (green, middle panels) or TuJ1 (green, right panels) and GFAP (red, right panels). Note that fewer *Bmi1*-deficient cells were TuJ1 positive. Nuclei were counterstained with DAPI (blue).

capable of transforming than LeX− fractions. But we did again observe a dramatic reduction in the number of TuJ1+ cells generated, both from LeX+ and LeX− *Bmi1*-deficient cells. Of note, under serum conditions, LeX+ fractions rapidly downregulated LeX expression (data not shown).

Bmi1-Deficient Astrocytes Have an Impaired Proliferative Response

For some experiments, instead of administering EGF, we overexpressed a constitutively active EGF receptor (EGFR) mutant. This EGFR (also EGFRvIII, ΔEGFR, or *EGFR), derived from human glioma, confers growth factor-independent growth on astrocytes (Bachoo et al., 2002; Ekstrand et al., 1992; Holland et al., 1998; Nishikawa et al., 1994). Under serum conditions, *Bmi1*$^{-/-}$*;Ink4a/Arf*$^{-/-}$ astrocytes transduced with either empty vector or *EGFR retrovirus proliferate at a significantly lower rate (Figure S5A). Measuring BrdU uptake during *EGFR-induced transformation in serum-free conditions also revealed a delayed proliferative response in *Bmi1*$^{-/-}$*;Ink4a/Arf*$^{-/-}$ cells (Figure S5B). Since *Bmi1* represses *Ink4a/Arf*, we tested whether *Bmi1* absence induces other cell cycle inhibitors. We could not find an increase in $p15^{Ink4a}$, $p21^{cip1}$, $p27^{kip1}$, or p53 proteins (Figure S5C), nor could we detect any changes in mRNA levels for $p15^{Ink4b}$, $p18^{Ink4c}$, or $p19^{Ink4d}$ (data not shown). We did notice that in the absence of *Bmi1*, endogenous EGFR levels were increased (Figure S5D).

To rule out the possibility of improper EGFR expression, we overexpressed either wild-type (WT) or *EGFR in *Bmi1*$^{-/-}$*;Ink4a/Arf*$^{-/-}$ astrocytes (Figure S5F), but transformation was still impaired (Figure S5E). Next, we overexpressed different combinations of effector domain mutants of oncogenic H-Ras in *Ink4a/Arf*$^{-/-}$ control cells (Figure S6B) (Rangarajan et al., 2004; Rodriguez-Viciana et al., 1997) and observed that activation of at least two known EGFR downstream pathways (Ral-GEF or PI3 kinase activation together with Raf pathway activation) is sufficient to induce transformation (Figure S6A). But as assessed by ERK, Akt, or FAK phosphorylation, downstream effectors were not differentially activated by EGF in *Bmi1* null cells, indicating that no common EGFR targets are mediating the phenotype (Figures S5G and S6E). Lastly, we established that inhibition of transformation of *Bmi1*$^{-/-}$*;Ink4a/Arf*$^{-/-}$ astrocytes is not EGFR specific since these cells are also resistant against H-RasV12 or TrkB/BDNF induced transformation (Figures S6C and S6D). However, these transformation defects are cell type specific as we also performed a number of transformation assays on embryonic mouse fibroblasts, but here, we did not find any differences (Figure S7).

BMI1 Is Expressed in Human Glioma and Required for In Vivo Transformation and Differentiation of *Ink4a/Arf*-Deficient Astrocytes

In normal human brain, we find nuclear BMI1 expression in the vast majority of cells (Figure 3A) similar to mice.

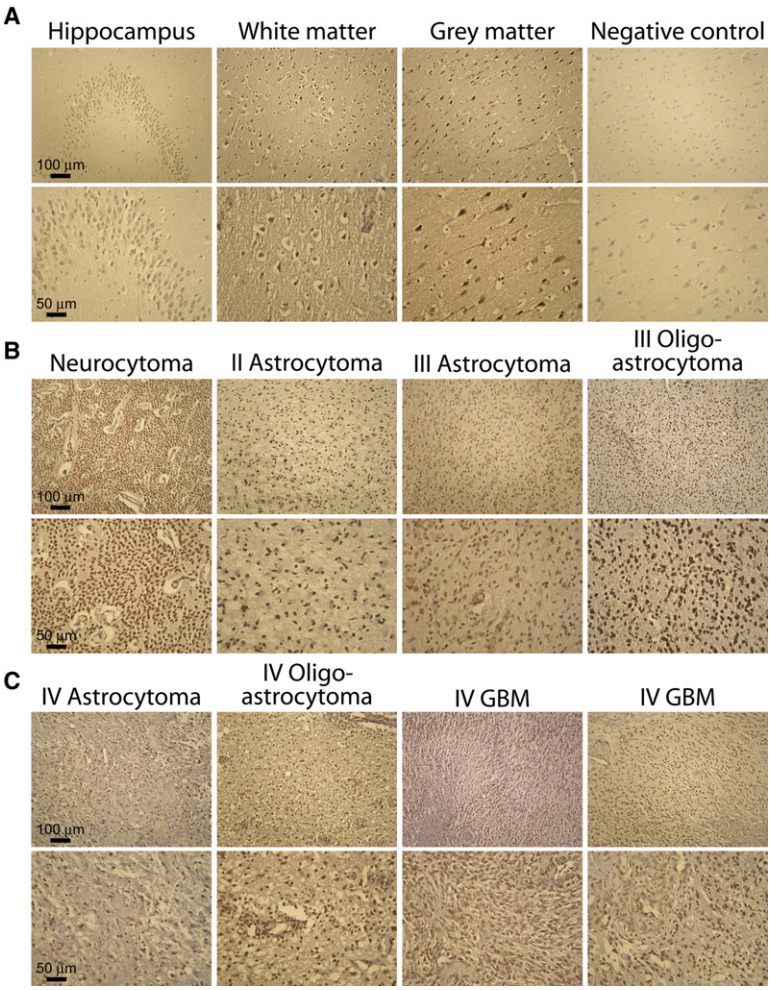

Figure 3. BMI1 Is Widely Expressed in Normal Human Brain Tissue and Brain Tumors

(A) Immunohistochemical staining for BMI1 in different areas of the human brain.

(B and C) Immunohistochemical staining for BMI1 in human neurocytoma and low-grade glioma (B) and in high-grade glioma (C).

Substantiating the idea that *BMI1* has a function in human glioma is the finding that the protein is expressed in almost all human brain tumors analyzed, such as lower grade astro-, oligo-, or oligoastrocytomas and neurocytomas (Figure 3B) and in high-grade gliomas and GBM (Figure 3C).

To demonstrate that *Bmi1* modulates in vivo gliomagenesis, we made use of an orthotopic transplantation model in which *EGFR drives tumor growth of primary astrocytes (Bachoo et al., 2002). *(Bmi1$^{-/-}$;)Ink4a/Arf$^{-/-}$* *EGFR (or empty vector as control) astrocytes (Figure 4C) were stereotactically intracranially injected and allowed up to 4 months to form tumors (Figure 4A). In addition, these cells were labeled with an EGFP-IRES-Luciferase construct that allowed us to follow tumor growth noninvasively in vivo. We measured the time between tumor cell injection and lethal tumor development and noticed a dramatic prolongation of the survival of mice injected with *Bmi1$^{-/-}$;Ink4a/Arf$^{-/-}$* cells (Figure 4B), indicating that *Bmi1* facilitates tumor formation. Notably, empty vector-transduced astrocytes do not form tumors, demonstrating they are not tumorigenic. Using in vivo bioluminescence, we observed a trend in which *Ink4a/Arf$^{-/-}$* *EGFR cells immediately formed tumors, while *Bmi1$^{-/-}$;Ink4a/Arf$^{-/-}$* *EGFR cells first went through a lag phase (Figure 4D). Finally, tumor samples were stained for a number of molecular markers and histologically analyzed by pathologists (Figure 4E). They resembled human glioma, with the exception that hyperproliferation of the endothelium was only rarely present. Both *Ink4a/Arf$^{-/-}$* and *Bmi1$^{-/-}$;Ink4a/Arf$^{-/-}$* tumors developed into grade III–IV (oligo)astrocytomas or GBM, whereby *Bmi1$^{-/-}$;Ink4a/Arf$^{-/-}$* tumors exhibited more pronounced pseudopalisading around micronecrotic areas. We did not find any differences in proliferation in the tumors as determined by PCNA positivity (Figures S8A and S8B). In line with the presence of stem cell-like cells, human GBM regularly exhibit glial and neuronal differentiation in combination with expression of primitive markers. Corroborating this, we found that the majority *Ink4a/Arf$^{-/-}$* tumors exhibited immunopositive areas for the progenitor marker Nestin (8/8), neuronal marker TuJ1 (5/8), and patchy staining for astrocytic marker GFAP (8/8) (Figure 4E). In contrast, only 3 out of 6 *Bmi1$^{-/-}$;Ink4a/Arf$^{-/-}$* tumors were positive for Nestin, and only 1 tumor expressed TuJ1.

One explanation for the differences in tumor development could be that the number of cells capable of growing out into a tumor (i.e., the number of tumor-forming cells) differs between *Ink4a/Arf*$^{-/-}$ and *Bmi1*$^{-/-}$*;Ink4a/Arf*$^{-/-}$ cultures. To address this, we isolated genomic DNA from the preinjected cells and from tumor-derived cells and performed Southern blot analysis (Figure S9). We made use of the fact that the cultures originally had been transduced with *EGFR-Blasticidin containing retroviruses at an MOI of 1. Hence, we reasoned that each cell must have one unique integration, with the result that the polyclonal preinjected populations should appear as a smear on the blot when visualized with a probe against the Blasticidin resistance gene. Consequently, if any selection had occurred during the process of tumor formation, the tumor-derived cell populations would give a banded pattern. This is exactly what we observed, and importantly, there are no differences between the number of bands of *Ink4a/Arf*$^{-/-}$ versus *Bmi1*$^{-/-}$*;Ink4a/Arf*$^{-/-}$ cultures, indicating that approximately equal numbers of tumor-forming cells were present.

Glial Cells Deficient for *Bmi1* Undergo Significant Changes in Gene Expression during Tumorigenesis

The increased survival of mice receiving *Bmi1*$^{-/-}$*;Ink4a/Arf*$^{-/-}$ cells together with the bioluminescence data suggesting a lag phase before tumor formation led us to speculate that *Bmi1*-deficient cells undergo substantial changes in gene expression before emerging into tumors. To investigate this, we isolated cells from tumors and compared their gene expression profile to the original preinjected tumor-inducing cells using oligo-microarrays. The control hybridizations (*Ink4a/Arf*$^{-/-}$ *EGFR, n = 3 independent tumors) yielded an average of 601 outliers (Figure 5A). In contrast, when hybridizing *Bmi1*$^{-/-}$*;Ink4a/Arf*$^{-/-}$ cells (n = 6 independent tumors), we obtained an average of 2950 outliers per experiment substantiating our presumption. Next, we did clustering analysis on the common outliers of the control and *Bmi1*$^{-/-}$*;Ink4a/Arf*$^{-/-}$ array experiments using Genesis software (Figures 5B and 5D) (Sturn et al., 2002). The *Ink4a/Arf*$^{-/-}$ control arrays only had 54 outliers in common clustering into no obvious patterns, whereas the common outliers from the *Bmi1*$^{-/-}$*;Ink4a/Arf*$^{-/-}$ arrays (551 in total) strongly clustered and were consistently up- or downregulated. These data suggest that *Bmi1*-deficient cells not only undergo significantly more changes in gene expression during tumor growth, but that they need to change expression of a specific group of genes to compensate for *Bmi1* absence. To obtain insight into the affected pathways, we analyzed the data from three control versus three experimental arrays using Ingenuity Pathway Analysis software (Ingenuity Systems, Redwood City, CA). This program translates array data into ontological (functionally related) groups. In Figure 5C, we show the eight most and two least significantly affected groups in the *Bmi1*$^{-/-}$*;Ink4a/Arf*$^{-/-}$ arrays. Most striking were "Cellular Movement," "Growth and Proliferation," and "Tissue Development."

Bmi1-Deficient Neural Stem Cells Give Rise to Lower Grade Glioma and Have Reduced Differentiation Capacity

Next, we set out to demonstrate that NSCs, another candidate "cell type of origin" for GBM, require *Bmi1* for tumor development. For this purpose, we isolated primary NSCs from *Ink4a/Arf*$^{-/-}$ or *Bmi1*$^{-/-}$*;Ink4a/Arf*$^{-/-}$ adult mouse SVZ. Importantly, we maintained these cells as monolayers on poly-L-Ornithine and Laminin coated dishes (Conti et al., 2005). Under serum-free stem cell conditions, these cultures were 100% Nestin and LeX positive and completely negative for GFAP and TuJ1, implying a high degree of homogeneity (Figures S10A–S10D). When induced to differentiate with 2% FBS for 7 days, both *Ink4a/Arf*$^{-/-}$ and *Bmi1*$^{-/-}$*;Ink4a/Arf*$^{-/-}$ NSCs efficiently generated GFAP- and TuJ1-positive cells while completely switching off Nestin (Figure 6D, Figures S10E and S10F). They were transduced with empty vector or *EGFR (Figure 6B) and subsequently stereotactically injected into the brain. Similar to the astrocyte experiments, we observed a significant increase in survival of mice receiving *Bmi1*$^{-/-}$*;Ink4a/Arf*$^{-/-}$ cells (Figure 6A), confirming that *Bmi1* facilitates a rapid onset of tumor growth. Also, there was no difference in proliferation rate between the tumors at the time of death (Figures S8C and S8D). But unlike the astrocyte-derived tumors, we did not find any GBM among the *Bmi1*$^{-/-}$*;Ink4a/Arf*$^{-/-}$ panel when we analyzed the tumors histologically, whereas a number of control tumors was diagnosed as such (Figure 6C). Also, none of the *Bmi1*-deficient tumors exhibited pseudopalisading. This suggests that in the absence of *Bmi1*, NSCs may not become fully malignant. Immunostainings for Nestin, GFAP, and TuJ1 revealed more differences (Figure 6C). Both types of tumors were consistently positive for GFAP, but while all *Ink4a/Arf*$^{-/-}$ tumors (7/7) were positive for Nestin, only half of the *Bmi1*$^{-/-}$*;Ink4a/Arf*$^{-/-}$ tumors (4/7) showed Nestin staining. Even more striking, the majority of *Ink4a/Arf*$^{-/-}$ (5/7) tumors strongly expressed neuronal marker TuJ1 versus 1/7 *Bmi1*$^{-/-}$*;Ink4a/Arf*$^{-/-}$ tumors. All tumors were negative for Neurofilament and Synaptophysin, while some but not all TuJ1+ tumors stained positive for MAP2 (data not shown).

We next asked the question whether *Bmi1*$^{-/-}$*;Ink4a/Arf*$^{-/-}$ NSCs also would have impaired neurogenic capacity. Up to 10 passages (approximately 3 weeks) following isolation, we could not detect any differences in neurogenic capacity between *Ink4a/Arf*$^{-/-}$ and *Bmi1*$^{-/-}$*;Ink4a/Arf*$^{-/-}$ NSCs (Figure 6D). However, at later time points, *Bmi1*$^{-/-}$*;Ink4a/Arf*$^{-/-}$ NSCs lost their ability to efficiently generate TuJ1+ neurons and GFAP+ astrocytes, whereas control NSCs continued to do so up to at least 30 passages (Figures 6E and 6F; Figure S10G). Notably, both control and *Bmi1*-deficient NSC cultures remained completely positive for Nestin under stem cell conditions (Figure 6E).

Altogether, these data demonstrate that *Bmi1* is essential for the development of high-grade glioma from NSCs and that multipotency becomes lost in the absence of *Bmi1*, both in vitro and in vivo.

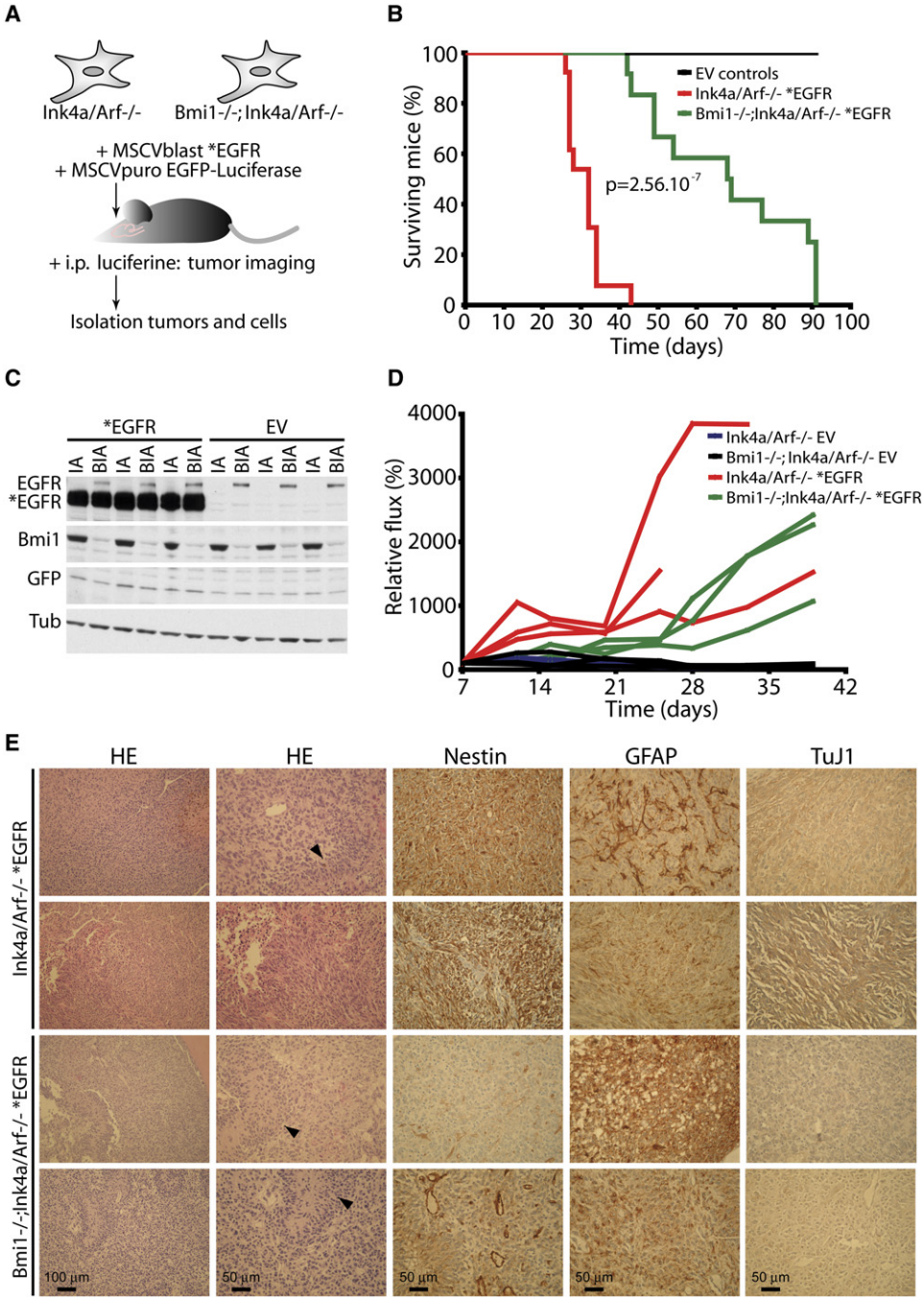

Figure 4. *Bmi1* Is Required for *Ink4a/Arf*$^{-/-}$ Astrocyte Transformation In Vivo

(A) Experimental set up: *Ink4a/Arf*$^{-/-}$ or *Bmi1*$^{-/-}$;*Ink4a/Arf*$^{-/-}$ primary astrocytes were transduced with retroviruses containing no insert (empty vector control, EV) or mutant EGFR (*EGFR) and cotransduced with an EGFP-IRES-Luciferase construct. Cells were stereotactically injected into the right hemisphere of nude mice. At specific time points, tumor mass was determined by intraperitoneal injection of luciferine followed by quantification of the amount of light emitted. When mice showed signs of tumor development, tumors were isolated for histological analysis or derivation of cell cultures.

(B) Mice injected with *Ink4a/Arf*$^{-/-}$ *EGFR astrocytes (n = 13) developed brain tumors between 26 and 43 days following injection, and mice injected with *Bmi1*$^{-/-}$;*Ink4a/Arf*$^{-/-}$ *EGFR astrocytes (n = 12) developed brain tumors significantly later, between 42 and 91 days (log-rank test, $p = 2.56 \times 10^{-7}$). Mice injected with either *Ink4a/Arf*$^{-/-}$ EV (n = 5) or *Bmi1*$^{-/-}$;*Ink4a/Arf*$^{-/-}$ EV astrocytes (n = 5) did not develop tumors.

(C) Western blot demonstrating equal *EGFR and EGFP expression levels in *Ink4a/Arf*$^{-/-}$ (IA) or *Bmi1*$^{-/-}$;*Ink4a/Arf*$^{-/-}$ (BIA) astrocytes used for stereotactic injections (shown are representative examples of different injected cell lines). Tub, alpha tubulin.

(D) Live imaging of tumor development by measuring bioluminescence of *Ink4a/Arf*$^{-/-}$ *EGFR versus *Bmi1*$^{-/-}$;*Ink4a/Arf*$^{-/-}$ *EGFR tumors in time. A trend was observed in which *Bmi1*$^{-/-}$;*Ink4a/Arf*$^{-/-}$ tumors developed with a later onset than control tumors. Each line represents tumor growth kinetics for one mouse, depicted are three representative examples for each experimental group.

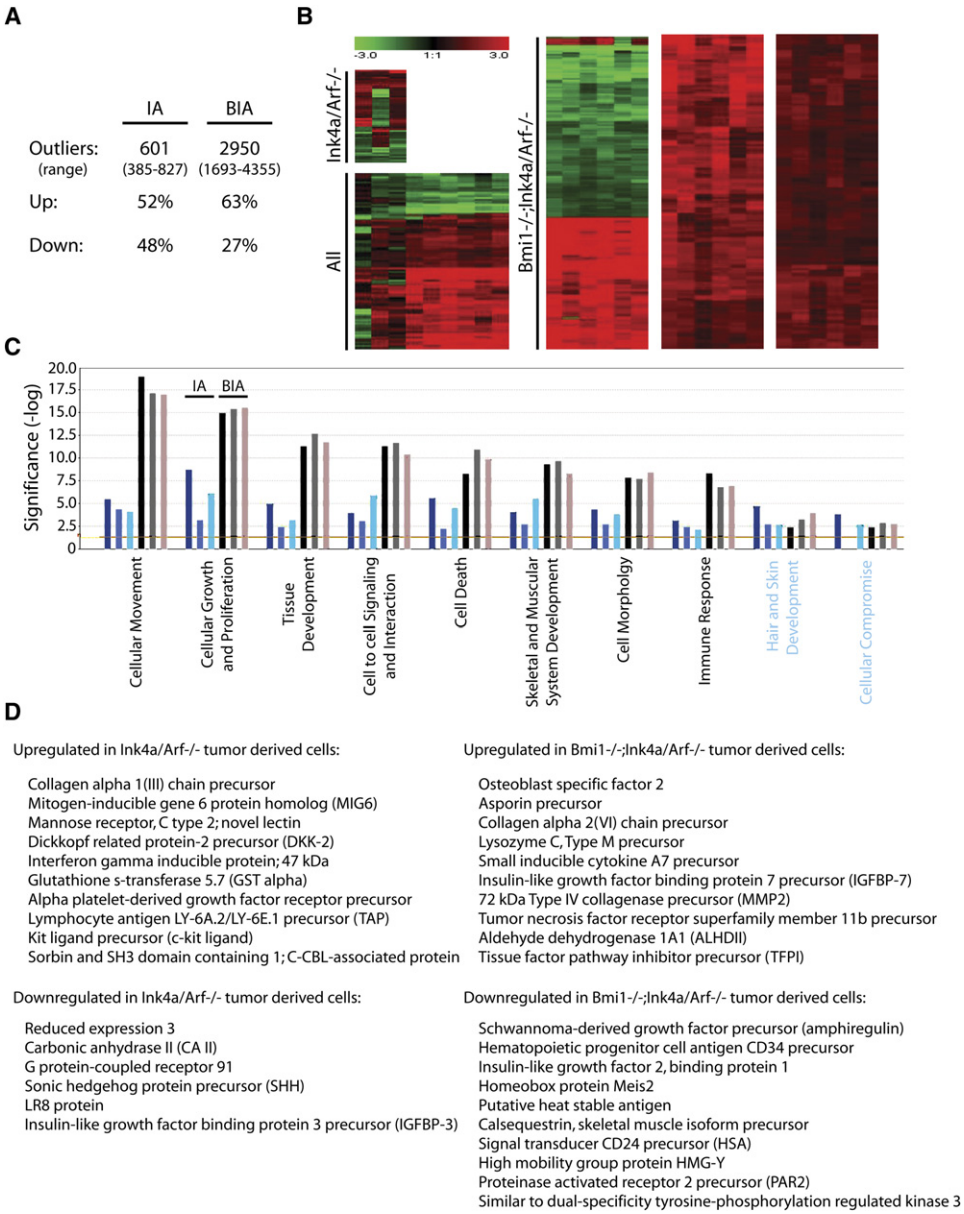

Figure 5. *Bmi1*$^{-/-}$;*Ink4a/Arf*$^{-/-}$ *EGFR Astrocyte-Derived Tumor Cell Lines Have Undergone Substantial Changes in Gene Expression

(A) Comparison of total outlier number between *(Bmi1*$^{-/-}$*;)Ink4a/Arf*$^{-/-}$ *EGFR preinjected and tumor-derived cell lines (n = 3 and 6 experiments, respectively). Shown are the average numbers of outliers (range). Up indicates upregulated in the tumor cells.

(B) Clustering analysis of common outliers (n = 54 for the *Ink4a/Arf*$^{-/-}$ *EGFR arrays versus n = 551 for *Bmi1*$^{-/-}$*;Ink4a/Arf*$^{-/-}$ *EGFR arrays) demonstrates that *Bmi1*$^{-/-}$*;Ink4a/Arf*$^{-/-}$ *EGFR tumor cells consistently change their gene expression profile upon injection and tumor growth. A red signal indicates higher gene expression in the tumor cells compared to the preinjected astrocytes, and green indicates lower gene expression. Note that we applied less stringent criteria when combining all nine arrays ($p > 0.01$ allowed for 1 data point).

(C) Ontological pathway analysis reveals the 8 most (black text) and 2 least (blue text) significantly altered ontological gene groups upon tumor development from *Bmi1*$^{-/-}$*;Ink4a/Arf*$^{-/-}$ cells. n = 3 *Ink4a/Arf*$^{-/-}$ (IA) versus n = 3 *Bmi1*$^{-/-}$*;Ink4a/Arf*$^{-/-}$ (BIA) arrays.

(D) List of the most significantly up- and downregulated genes in the *Ink4a/Arf*$^{-/-}$ *EGFR and *Bmi1*$^{-/-}$*;Ink4a/Arf*$^{-/-}$ *EGFR arrays.

(E) Histological analysis of astrocyte-derived brain tumors. Depicted are two representative examples from each experimental group. Both *Ink4a/Arf*$^{-/-}$ *EGFR and *Bmi1*$^{-/-}$*;Ink4a/Arf*$^{-/-}$ *EGFR tumors were classified as grade III anaplastic (oligo)astrocytomas or grade IV glioblastomas multiforme (HE panels). Pseudopalisading (indicated by arrowheads) was more pronounced in *Bmi1*$^{-/-}$*;Ink4a/Arf*$^{-/-}$ tumors. 8/8 *Ink4a/Arf*$^{-/-}$ tumors showed strong Nestin positivity compared to 3/6 *Bmi1*$^{-/-}$*;Ink4a/Arf*$^{-/-}$ tumors (Nestin panels). 5/8 *Ink4a/Arf*$^{-/-}$ tumors were positive for the neuronal marker TuJ1 versus 1/6 *Bmi1*$^{-/-}$*;Ink4a/Arf*$^{-/-}$ tumors (TuJ1 panels). GFAP staining was patchy and similar between the two experimental groups (GFAP panels). HE, hematoxylin & eosin; TuJ1, β-tubulin III.

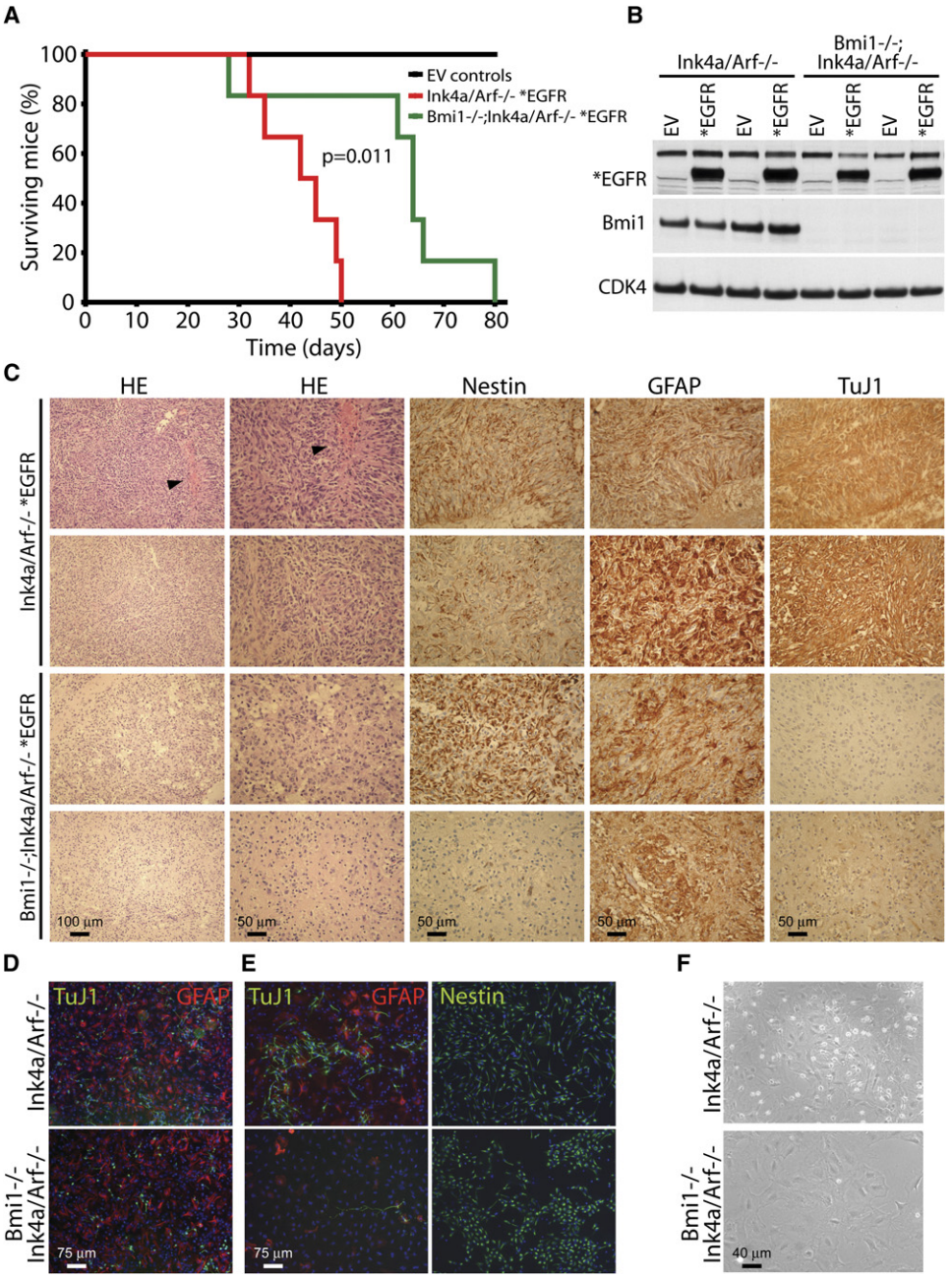

Figure 6. *Bmi1* Is Required for *Ink4a/Arf*$^{-/-}$ Neural Stem Cell Transformation In Vivo

(A) Mice stereotactically injected with *Ink4a/Arf*$^{-/-}$ *EGFR primary neural stem cells (n = 7) develop brain tumors between 32 and 50 days following injection, mice injected with *Bmi1*$^{-/-}$;*Ink4a/Arf*$^{-/-}$ *EGFR cells (n = 7) develop brain tumors significantly later between 28 and 80 days (log-rank test, p = 0.011). Mice receiving either *Ink4a/Arf*$^{-/-}$ EV (n = 5) or *Bmi1*$^{-/-}$;*Ink4a/Arf*$^{-/-}$ EV (n = 8) cells developed no tumors.

(B) Western blot analysis demonstrates equal *EGFR expression levels in *Ink4a/Arf*$^{-/-}$ (IA) or *Bmi1*$^{-/-}$;*Ink4a/Arf*$^{-/-}$ (BIA) stem cells (shown are representative examples of different injected cell lines). CDK4, loading control.

(C) Histological analysis of NSC-derived brain tumors. Depicted are two representative examples from each experimental group. Both *Ink4a/Arf*$^{-/-}$ *EGFR and *Bmi1*$^{-/-}$;*Ink4a/Arf*$^{-/-}$ *EGFR tumors contained grade III anaplastic (oligo)astrocytomas. However, in contrast to the *Bmi1*$^{-/-}$;*Ink4a/Arf*$^{-/-}$ *EGFR tumors, the majority of *Ink4a/Arf*$^{-/-}$ *EGFR tumors showed clear pseudopalisading (arrowheads) and appeared more aggressive. Some *Ink4a/Arf*$^{-/-}$ tumors were classified as grade IV glioblastoma multiforme (HE panels). 7/7 *Ink4a/Arf*$^{-/-}$ tumors showed strong Nestin positivity compared to 4/7 *Bmi1*$^{-/-}$;*Ink4a/Arf*$^{-/-}$ tumors (Nestin panels). 5/7 *Ink4a/Arf*$^{-/-}$ tumors were positive for the neuronal marker TuJ1 versus 1/7 *Bmi1*$^{-/-}$;*Ink4a/Arf*$^{-/-}$ tumors (TuJ1 panels). GFAP staining was similar between the two experimental groups (GFAP panels).

(D) Primary NSCs (up to 3 weeks following isolation) were induced to differentiate with 2% FBS for 7 days and stained for TuJ1 (green) or GFAP (red). Nuclei were counterstained with DAPI (blue).

DISCUSSION

Because of the many similarities between cancer and normal stem cells, one can assume that processes regulating stem cell proliferation and maintenance are also fundamental to cancer stem cells. We attempted to elucidate the role of PcG gene *Bmi1* in the formation of glioblastoma multiforme, one of the cancers driven by a cancer stem cell subpopulation (Galli et al., 2004; Hemmati et al., 2003; Singh et al., 2004). *Bmi1* has been demonstrated to be essential for the proliferation and self-renewal of leukemic stem cells (Lessard and Sauvageau, 2003), as well as normal neural stem cells by repressing the *Ink4a/Arf* locus (Bruggeman et al., 2005; Molofsky et al., 2005). In this study, we extended our scope and specifically searched for *Ink4a/Arf*-independent functions of *Bmi1* in brain cancer.

Bmi1 Is Required for Proliferation and Transformation of Primary Glial Cells

We used an established orthotopic transplantation model to study transformation of brain cells in vitro and in vivo. Taking into account that the cell-of-origin for glioma (stem) cells is not necessarily a differentiated glial cell and that *Bmi1* is expressed in the vast majority of brain cells, we aimed at analyzing the capacity of both primary astrocytes and NSCs deficient for *Ink4a/Arf* to transform upon EGF overstimulation in the absence of *Bmi1*. We would like to note that, while we have attempted to establish pure astrocyte and neural stem cell cultures in compliance with published methods, the current lack of markers definitively distinguishing between terminally differentiated astrocytes and more primitive ancestors urges for some reticence when using these terms.

The induction of Bmi1 protein during in vitro transformation already hinted at a role for *Bmi1* in this process. Indeed, whereas control *Ink4a/Arf*$^{-/-}$ astrocytes rapidly undergo morphological changes typical of transformation such as loss of contact inhibition and acquisition of anchorage independent growth, in the absence of *Bmi1*, these cells virtually lose this capacity. This is cell type specific as there was no such difference in transforming capacity of mouse fibroblasts. A number of alterations in cell physiology have been proposed to be essential for malignant growth (Hanahan and Weinberg, 2000). Among these are self-sufficiency in growth signals, limitless replicative potential, insensitivity to growth-inhibitory signals, and tissue invasion and metastasis. The first two requirements are met by presence of *EGFR and deletion of *Ink4a/Arf*. The reduced proliferative activity of *Bmi1*$^{-/-}$*;Ink4a/Arf*$^{-/-}$ astrocytes may compromise the third hallmark and thus underlie the transformation defect. However, negation to change growth mode from adherent toward anchorage-independent suggests that pathways implicated in cell-cell and cell-matrix interactions are impaired as well, and this could impair the fourth trait. Curiously, *Bmi1*$^{-/-}$*;Ink4a/Arf*$^{-/-}$ astrocytes can survive and grow in suspension when plated onto ultra low-binding plates (S.B. and M.v.L., unpublished data), indicating a preference to grow adherent rather than a complete incapability to do so. Altering adhesive properties can be beneficial to tumor cells in different ways. First, loss of anchorage dependence protects cells from anoikis and facilitates survival during metastasis. Second, invasion and migration through the stroma entails both adhesion and remodeling of the extracellular matrix (Gupta and Massague, 2006). Notably, extensive migration throughout the brain is a principal feature of malignant glioma (Giese et al., 2003). In concert with our gene expression studies revealing specific changes in adhesion-related pathways in *Bmi1*$^{-/-}$*;Ink4a/Arf*$^{-/-}$ tumor cells, we propose that *Bmi1*-deficient cells are less tumorigenic due to a combination of altered proliferative and adhesive properties.

Bmi1-Deficiency Impedes Tumor Growth and Biases toward a Less Malignant Phenotype

By intracranial injection of astrocytes and NSCs, we were able to disclose a number of differences between tumors derived from *Ink4a/Arf*$^{-/-}$ and *Bmi1*$^{-/-}$*;Ink4a/Arf*$^{-/-}$ cells in vivo. Both when using astrocytes and NSCs, we observed a dramatic increase in survival of mice receiving *Bmi1*-deficient cells. This can be explained by a general reduction in tumor cell proliferation; however, no such differences were evident at the time of death. An alternative explanation could be a difference in the number of "tumor-initiating" cells present in *Ink4a/Arf*$^{-/-}$ and *Bmi1*$^{-/-}$*;Ink4a/Arf*$^{-/-}$ cell cultures, but Southern blot analysis demonstrating equal amounts of cells contributing to tumorigenesis argues against this. Another possibility is that *Bmi1* knockout cells require a substantial amount of time to adapt their gene expression such that a tumor can form. This hypothesis is supported by the in vivo bioluminescence data portraying the *Bmi1*$^{-/-}$*;Ink4a/Arf*$^{-/-}$ tumors as residing in an initial phase of slow growth before emerging into a tumor. Corroborating this, comparison of gene expression profiles between preinjected and tumor cells clearly showed that *Bmi1*$^{-/-}$*;Ink4a/Arf*$^{-/-}$ cells have undergone significantly larger alterations in transcription than control cells, and a core group of perfectly clustering genes can easily be distilled. This "*Bmi1* null profile" can be dissected into a number of interesting gene networks. Most outstanding is the "Cellular Movement" cluster comprising cell movement, migration, chemotaxis, and homing. This is well in accordance with our finding that *Bmi1*-deficient astrocytes in culture exhibit impaired

(E) NSCs between 3 and 10 weeks following isolation under stem cell conditions were stained for Nestin (green, right panels). They were differentiated with 2% FBS for 7 days and stained for TuJ1 (green, left panels) or GFAP (red, left panels). Note the reduced generation of TuJ1+ cells in the absence of *Bmi1*. Nuclei were counterstained with DAPI (blue).
(F) Phase contrast photographs of differentiated NSCs between 3–10 weeks following isolation showing fewer cells with neuronal morphology in the absence of *Bmi1*.

adhesive properties. Another significant cluster is "Cellular Growth and Proliferation," encompassing networks involved in proliferation and colony formation. Again, this is in agreement with our in vitro observation that EGF-stimulated *Bmi1*$^{-/-}$;*Ink4a/Arf*$^{-/-}$ cells initially have a reduced proliferative response. A role for a PcG gene in adhesion is not without precedent. A recent study demonstrated the involvement of *Ezh2* in the dynamics of the cytoskeleton (Su et al., 2005). As *Ezh2* also stimulates proliferation, regulating proliferation and adhesion could be a universal PcG feature.

Because the *Bmi1*-deficient tumors arose at a later time point, we anticipated they would differ histologically and possibly also in terms of malignancy. Here, a difference between the astrocyte- and NSC-derived tumors became apparent. Both *Bmi1*-deficient and -proficient astrocytes gave at approximately equal ratios rise to gliomas, which according to pathologists, could be classified as grade III anaplastic (oligo)astrocytomas or grade IV GBM. Pseudopalisades, a typical feature of high-grade glioma, were detected in all GBM-classified tumors. In contrast, *Bmi1*-deficient NSCs never developed into tumors higher graded than III and on no account showed pseudopalisading, whereas control cells readily did. Additionally, *Bmi1*$^{-/-}$;*Ink4a/Arf*$^{-/-}$ NSC tumors appeared histologically distinct as they never exhibited extracranial growth but instead spread widely through the hemispheres. This discrepancy could relate to the cell-of-origin issue as, apparently, astrocytes respond differently to *Bmi1* absence than NSCs. Previous studies have ascribed more importance to *Bmi1* function in (cancer) stem cells than differentiated cells (Hosen et al., 2007; Liu et al., 2006; Molofsky et al., 2003; Prince et al., 2007). However, in addition to our observations that *Bmi1* is abundantly expressed in most brain (cancer) cells, we find that *Bmi1* is essential for astrocyte proliferation, which strongly argues that *Bmi1* controls both stem cells and their progeny. Therefore, we would rather propose that either *Bmi1* has additional functions in stem cells or, alternatively, that stem cells are more reliant on common *Bmi1* functions.

Bmi1-Deficient Glial Cells and Tumors Exhibit Reduced Differentiation Capacity

Another altered ontological cluster in the *Bmi1* null common profile was related to development ("Tissue Development"). Knowing that PcG actively represses genes involved in fate choice during embryogenesis (Boyer et al., 2006; Bracken et al., 2006; Lee et al., 2006; Negre et al., 2006; Tolhuis et al., 2006), we questioned whether *Bmi1* deficiency would lead to alterations in differentiation status of the tumors. In accordance with a stem cell component, GBM cells sometimes differentiate toward the neuronal in addition to the glial lineage (Katsetos et al., 2001; Martinez-Diaz et al., 2003). Both our astrocyte- and NSC-derived control tumors were positive for Nestin, GFAP, and TuJ1, indicating that these tumors indeed differentiate into all lineages. But, GBMs can be infiltrated with reactive cells and are sometimes promiscuous in marker expression (Katsetos et al., 2001; Katsetos et al., 2004). Therefore, we interpret TuJ1 positivity as an attempt of the glioma cell to differentiate into the neuronal lineage but do not conclude presence of mature neurons from this. Nonetheless, it was striking that *Bmi1*$^{-/-}$;*Ink4a/Arf*$^{-/-}$ tumors stained less frequently positive for TuJ1, suggestive of impaired neuronal commitment. In addition, they less prominently expressed stem cell marker Nestin. One explanation for these observations is that in absence of *Bmi1*, the total number of primitive cells capable of differentiating is reduced due to impaired self-renewal. Alternatively, *Bmi1* is involved in the fate choice of the progenitor cell. It was already shown that *Bmi1*$^{-/-}$;*Ink4a/Arf*$^{+/+}$ neurospheres fail to efficiently produce neurons upon differentiation (Zencak et al., 2005). Also, neuroblastoma cells differentiating in culture and in tumors into Schwann-like cells (glial cell of the peripheral nervous system) show reduced Bmi1 protein expression, whereas cells differentiating into neuroblasts have higher levels of Bmi1 (Cui et al., 2006, 2007). Moreover, acute removal or overexpression of *Bmi1* in these cells instructed them to differentiate into the glial or neuronal lineage, respectively. Our in vitro experiments corroborate an *Ink4a/Arf*-independent role for *Bmi1* in differentiation, since both our *Bmi1*-deficient astrocytes and NSCs lost the capacity to generate neurons. It is conceivable that *Bmi1* has similar effects on GBM cells in vivo.

Altogether, the *Bmi1* characteristics described in this study have considerable implications for understanding PcG function in (stem) cells and cancer. Whereas previous attention was focused on repression of the *Ink4a/Arf* locus, we now clearly demonstrate that *Bmi1* also regulates alternative pathways involved in proliferation, adhesion, and differentiation. It is likely that these pathways are important both in the stem cell niche and in the process of tumor development, in particular in cancers associated with extensive migration and differentiation of tumor (stem) cells such as glioblastoma.

EXPERIMENTAL PROCEDURES

Mice Breeding, Tissue Isolation, and Preparation of Cell Cultures

Bmi1$^{-/-}$ (Van der Lugt et al., 1994) and *Ink4a/Arf*$^{-/-}$ mice (Serrano et al., 1996) were in an FVB background. For orthotopic transplantation studies, athymic (nude) FVB or Balb/c mice were used. Mice were killed by an overdose of CO_2 instantly followed by tissue isolation. NSCs and MEFs were isolated as described before (Bruggeman et al., 2005). NSCs were maintained in defined serum-free NSC medium containing 20 ng/ml EGF and 10 ng/ml bFGF (R&D systems) as adherent cultures on poly-L-Ornithine (15 μg/ml) and Laminin (5 μg/ml, both Sigma) coated plates (Conti et al., 2005). Primary astrocyte cultures were derived from 7-day-old mice using established methods (McCarthy and de Vellis, 1980). Briefly, neocortices were isolated and washed. Tissue was triturated, digested for 20 min at 37°C with Trypsin EDTA (Invitrogen)/DnaseI (Boehringer Mannheim) solution, and quenched with astrocyte culture medium (DMEM/F12, 10% FBS, Invitrogen). Cell suspensions were passed through cell strainers and plated in astrocyte culture medium.

All animal experiments were done conform national regulatory standards approved by the DEC (Animal Experiments Committee).

Expression Constructs, Virus Preparation, and Transductions

Human WT EGFR and *EGFR derived from pLWERNL and pLERNL, respectively (gift from Dr. W. Cavenee), were subcloned into retroviral expression vector pMSCV blasticidin. An MSCV puromycin (Clontech) construct containing Luciferase-IRES-GFP was provided by Dr. A. Berns. pBABEpuro TrkB and pBABEhygro BDNF were gifts from Dr. D. Peeper. H-RasV12 mutants (Rodriguez-Viciana et al., 1997) were subcloned into MSCVpuro. For knockdown experiments, a pRETRO-SUPER construct containing a sequence targeting *Bmi1* (GTATTGTCCTATTTGTGAT) was used.

For retroviral transductions, see the Supplemental Data.

Cell Culture Experiments

For 3T3 proliferation assays, cells were passaged every 3 days and counted. BrdU incorporation assays (1 hr pulse of 10 μM BrdU) were done as described before (Bruggeman et al., 2005).

In vitro astrocyte transformation was studied by plating 30,000 primary cells in 6-well plates. They were incubated in NSC medium containing 20 ng/ml EGF and scored for morphological changes after 14–15 days. For some experiments, EGF-induced cultures were switched to NSC medium containing 2% FBS for 7 days. For soft agar assays, 50,000 cells were seeded in 6-well plates in DMEM containing FBS and 0.35% agar. Colony formation was scored after 3 weeks.

In vitro NSC differentiation was studied by plating 150,000 (adherent) NSCs onto poly-L-Ornithine and Laminin coated coverslips in 6-well plates. They were incubated in NSC medium containing 2% FBS for 7 days.

To study phosphorylation, astrocytes were serum starved overnight and pulsed for 15 or 45 min with 20 ng/ml EGF or 10% FBS followed by immediate cell lysis in the presence of protease and phosphatase inhibitors.

Western Blot Analysis, Immunofluorescence, and Immunohistochemistry

Western blot analysis and immunofluorescence were done as described previously (Bruggeman et al., 2005). For LeX/SSEA-1/CD15 immunofluorescence, live cells were incubated with anti-LeX antibody for 30 min prior to fixation. For IHC stainings and antibodies, see the Supplemental Data. Anonymous human brain (tumor) samples were obtained from the Free University Medical Centre and the Sloter-vaart Hospital (Amsterdam, the Netherlands) in agreement with the national "code of adequate use of tissue," approved by the METC (medical-ethical review committee).

Stereotactic Brain Injections, Bioluminescence Imaging, and Tumor Collection

A detailed description of the stereotactic brain injection and bioluminescence procedures is given elsewhere (Kemper et al., 2006). In short, anaesthetized mice were placed in a stereotact and 100,000 cells were injected 2 mm lateral and 1 mm anterior to the bregma, 3 mm below the skull. For some experiments, tumor-bearing mice were injected intraperitoneally with 150 mg/kg luciferin (Xenogen), anaesthetized, and recorded within 10–20 min using a cooled IVIS camera (Xenogen Corp) twice a week. All mice were monitored for tumor development for a period of 4 months and sacrificed when they started to exhibit visible tumors or signs of sickness and weight loss. All organs were routinely analyzed to confirm the brain tumor to be the cause of death. Tumors were classified blindly by pathologists.

RNA Isolation, Quantitative Real-Time PCR, and Oligoarray Analysis

qRT-PCR was performed as before (Bruggeman et al., 2005). Protocols for oligoarray analysis can be downloaded from microarray.nki.nl. Expression data is available from the EBI ArrayExpress database (www.ebi.ac.uk/arrayexpress). EBI-ID: E-NCMF-4. See the Supplemental Data for details.

Supplemental Data

The Supplemental Data include ten supplemental figures and Supplemental Experimental Procedures and can be found with this article online at http://www.cancercell.org/cgi/content/full/12/4/328/DC1/.

ACKNOWLEDGMENTS

We thank A. Berns, W. Cavenee, R. DePinho, and D. Peeper for sharing reagents. We thank P. van der Valk, J. Westerga, and M. van der Valk for histological analysis and tissue samples. We are thankful to R. Kerkhoven, the NKI Central Microarray, Microscopy, FACS, and Animal Facilities for assistance with experiments. We thank N. Armstrong for statistical analysis and B. Westerman for critically reading the manuscript. S.B. is supported by grants from the Dutch Cancer Society and Hersenstichting to M.v.L.

Received: January 11, 2007
Revised: July 2, 2007
Accepted: August 29, 2007
Published: October 15, 2007

REFERENCES

Al Hajj, M., Wicha, M.S., Benito-Hernandez, A., Morrison, S.J., and Clarke, M.F. (2003). Prospective identification of tumorigenic breast cancer cells. Proc. Natl. Acad. Sci. USA *100*, 3983–3988.

Bachoo, R.M., Maher, E.A., Ligon, K.L., Sharpless, N.E., Chan, S.S., You, M.J., Tang, Y., DeFrances, J., Stover, E., Weissleder, R., et al. (2002). Epidermal growth factor receptor and Ink4a/Arf: Convergent mechanisms governing terminal differentiation and transformation along the neural stem cell to astrocyte axis. Cancer Cell *1*, 269–277.

Bonnet, D., and Dick, J.E. (1997). Human acute myeloid leukemia is organized as a hierarchy that originates from a primitive hematopoietic cell. Nat. Med. *3*, 730–737.

Boyer, L.A., Plath, K., Zeitlinger, J., Brambrink, T., Medeiros, L.A., Lee, T.I., Levine, S.S., Wernig, M., Tajonar, A., Ray, M.K., et al. (2006). Polycomb complexes repress developmental regulators in murine embryonic stem cells. Nature *441*, 349–353.

Bracken, A.P., Dietrich, N., Pasini, D., Hansen, K.H., and Helin, K. (2006). Genome-wide mapping of Polycomb target genes unravels their roles in cell fate transitions. Genes Dev. *20*, 1123–1136.

Bruggeman, S.W., Valk-Lingbeek, M.E., van der Stoop, P.P., Jacobs, J.J., Kieboom, K., Tanger, E., Hulsman, D., Leung, C., Arsenijevic, Y., Marino, S., and van Lohuizen, M. (2005). Ink4a and Arf differentially affect cell proliferation and neural stem cell self-renewal in Bmi1-deficient mice. Genes Dev. *19*, 1438–1443.

Conti, L., Pollard, S.M., Gorba, T., Reitano, E., Toselli, M., Biella, G., Sun, Y., Sanzone, S., Ying, Q.L., Cattaneo, E., and Smith, A. (2005). Niche-independent symmetrical self-renewal of a mammalian tissue stem cell. PLoS Biol. *3*, e283. 10.1371/journal.pbio.0030283.

Cui, H., Hu, B., Li, T., Ma, J., Alam, G., Gunning, W.T., and Ding, H.F. (2007). Bmi-1 is essential for the tumorigenicity of neuroblastoma cells. Am. J. Pathol. *170*, 1370–1378.

Cui, H., Ma, J., Ding, J., Li, T., Alam, G., and Ding, H.F. (2006). Bmi-1 Regulates the Differentiation and Clonogenic Self-renewal of I-type Neuroblastoma Cells in a Concentration-dependent Manner. J. Biol. Chem. *281*, 34696–34704.

Doetsch, F., Caille, I., Lim, D.A., Garcia-Verdugo, J.M., and Alvarez-Buylla, A. (1999). Subventricular zone astrocytes are neural stem cells in the adult mammalian brain. Cell *97*, 703–716.

Ekstrand, A.J., Sugawa, N., James, C.D., and Collins, V.P. (1992). Amplified and rearranged epidermal growth factor receptor genes in human glioblastomas reveal deletions of sequences encoding portions of the N- and/or C-terminal tails. Proc. Natl. Acad. Sci. USA *89*, 4309–4313.

Fomchenko, E.I., and Holland, E.C. (2006). Mouse models of brain tumors and their applications in preclinical trials. Clin. Cancer Res. *12*, 5288–5297.

Freedman, V.H., and Shin, S.I. (1974). Cellular tumorigenicity in nude mice: Correlation with cell growth in semi-solid medium. Cell *3*, 355–359.

Galli, R., Binda, E., Orfanelli, U., Cipelletti, B., Gritti, A., De Vitis, S., Fiocco, R., Foroni, C., Dimeco, F., and Vescovi, A. (2004). Isolation and characterization of tumorigenic, stem-like neural precursors from human glioblastoma. Cancer Res. *64*, 7011–7021.

Garcia, A.D., Doan, N.B., Imura, T., Bush, T.G., and Sofroniew, M.V. (2004). GFAP-expressing progenitors are the principal source of constitutive neurogenesis in adult mouse forebrain. Nat. Neurosci. *7*, 1233–1241.

Giese, A., Bjerkvig, R., Berens, M.E., and Westphal, M. (2003). Cost of migration: Invasion of malignant gliomas and implications for treatment. J. Clin. Oncol. *21*, 1624–1636.

Gupta, G.P., and Massague, J. (2006). Cancer metastasis: Building a framework. Cell *127*, 679–695.

Hanahan, D., and Weinberg, R.A. (2000). The hallmarks of cancer. Cell *100*, 57–70.

Haupt, Y., Alexander, W.S., Barri, G., Klinken, S.P., and Adams, J.M. (1991). Novel zinc finger gene implicated as myc collaborator by retrovirally accelerated lymphomagenesis in E mu-myc transgenic mice. Cell *65*, 753–763.

Hemmati, H.D., Nakano, I., Lazareff, J.A., Masterman-Smith, M., Geschwind, D.H., Bronner-Fraser, M., and Kornblum, H.I. (2003). Cancerous stem cells can arise from pediatric brain tumors. Proc. Natl. Acad. Sci. USA *100*, 15178–15183.

Holland, E.C., Hively, W.P., DePinho, R.A., and Varmus, H.E. (1998). A constitutively active epidermal growth factor receptor cooperates with disruption of G1 cell-cycle arrest pathways to induce glioma-like lesions in mice. Genes Dev. *12*, 3675–3685.

Hosen, N., Yamane, T., Muijtjens, M., Pham, K., Clarke, M.F., and Weissman, I.L. (2007). Bmi-1-green fluorescent protein-knock-in mice reveal the dynamic regulation of bmi-1 expression in normal and leukemic hematopoietic cells. Stem Cells *25*, 1635–1644.

Imura, T., Kornblum, H.I., and Sofroniew, M.V. (2003). The predominant neural stem cell isolated from postnatal and adult forebrain but not early embryonic forebrain expresses GFAP. J. Neurosci. *23*, 2824–2832.

Imura, T., Nakano, I., Kornblum, H.I., and Sofroniew, M.V. (2006). Phenotypic and functional heterogeneity of GFAP-expressing cells in vitro: Differential expression of LeX/CD15 by GFAP-expressing multipotent neural stem cells and non-neurogenic astrocytes. Glia *53*, 277–293.

Jacobs, J.J., Scheijen, B., Voncken, J.W., Kieboom, K., Berns, A., and van Lohuizen, M. (1999). Bmi-1 collaborates with c-Myc in tumorigenesis by inhibiting c-Myc-induced apoptosis via INK4a/ARF. Genes Dev. *13*, 2678–2690.

Katsetos, C.D., Del Valle, L., Geddes, J.F., Assimakopoulou, M., Legido, A., Boyd, J.C., Balin, B., Parikh, N.A., Maraziotis, T., de Chadarevian, J.P., et al. (2001). Aberrant localization of the neuronal class III beta-tubulin in astrocytomas. Arch. Pathol. Lab. Med. *125*, 613–624.

Katsetos, C.D., de Chadarevian, J.P., Legido, A., Perentes, E., and Mork, S.J. (2004). Giant cell glioblastoma and pleomorphic xanthoastrocytoma. Arch. Pathol. Lab. Med. *128*, 391–392.

Kemper, E.M., Leenders, W., Kusters, B., Lyons, S., Buckle, T., Heerschap, A., Boogerd, W., Beijnen, J.H., and van Tellingen, O. (2006). Development of luciferase tagged brain tumour models in mice for chemotherapy intervention studies. Eur. J. Cancer *42*, 3294–3303.

Kleihues, P., Louis, D.N., Scheithauer, B.W., Rorke, L.B., Reifenberger, G., Burger, P.C., and Cavenee, W.K. (2002). The WHO classification of tumors of the nervous system. J. Neuropathol. Exp. Neurol. *61*, 215–225.

Lapidot, T., Sirard, C., Vormoor, J., Murdoch, B., Hoang, T., Caceres-Cortes, J., Minden, M., Paterson, B., Caligiuri, M.A., and Dick, J.E. (1994). A cell initiating human acute myeloid leukaemia after transplantation into SCID mice. Nature *367*, 645–648.

Laywell, E.D., Rakic, P., Kukekov, V.G., Holland, E.C., and Steindler, D.A. (2000). Identification of a multipotent astrocytic stem cell in the immature and adult mouse brain. Proc. Natl. Acad. Sci. USA *97*, 13883–13888.

Lee, T.I., Jenner, R.G., Boyer, L.A., Guenther, M.G., Levine, S.S., Kumar, R.M., Chevalier, B., Johnstone, S.E., Cole, M.F., Isono, K., et al. (2006). Control of developmental regulators by Polycomb in human embryonic stem cells. Cell *125*, 301–313.

Lessard, J., and Sauvageau, G. (2003). Bmi-1 determines the proliferative capacity of normal and leukaemic stem cells. Nature *423*, 255–260.

Leung, C., Lingbeek, M., Shakhova, O., Liu, J., Tanger, E., Saremaslani, P., van Lohuizen, M., and Marino, S. (2004). Bmi1 is essential for cerebellar development and is overexpressed in human medulloblastomas. Nature *428*, 337–341.

Liu, L., Andrews, L.G., and Tollefsbol, T.O. (2006). Loss of the human Polycomb group protein BMI1 promotes cancer-specific cell death. Oncogene *25*, 4370–4375.

Martinez-Diaz, H., Kleinschmidt-DeMasters, B.K., Powell, S.Z., and Yachnis, A.T. (2003). Giant cell glioblastoma and pleomorphic xanthoastrocytoma show different immunohistochemical profiles for neuronal antigens and p53 but share reactivity for class III beta-tubulin. Arch. Pathol. Lab. Med. *127*, 1187–1191.

McCarthy, K.D., and de Vellis, J. (1980). Preparation of separate astroglial and oligodendroglial cell cultures from rat cerebral tissue. J. Cell Biol. *85*, 890–902.

Molofsky, A.V., Pardal, R., Iwashita, T., Park, I.K., Clarke, M.F., and Morrison, S.J. (2003). Bmi-1 dependence distinguishes neural stem cell self-renewal from progenitor proliferation. Nature *425*, 962–967.

Molofsky, A.V., He, S., Bydon, M., Morrison, S.J., and Pardal, R. (2005). Bmi-1 promotes neural stem cell self-renewal and neural development but not mouse growth and survival by repressing the p16Ink4a and p19Arf senescence pathways. Genes Dev. *19*, 1432–1437.

Negre, N., Hennetin, J., Sun, L.V., Lavrov, S., Bellis, M., White, K.P., and Cavalli, G. (2006). Chromosomal distribution of PcG proteins during Drosophila development. PLoS Biol. *4*, e170. 10.1371/journal.pbio.0040170.

Nishikawa, R., Ji, X.D., Harmon, R.C., Lazar, C.S., Gill, G.N., Cavenee, W.K., and Huang, H.J. (1994). A mutant epidermal growth factor receptor common in human glioma confers enhanced tumorigenicity. Proc. Natl. Acad. Sci. USA *91*, 7727–7731.

Park, I.K., Qian, D., Kiel, M., Becker, M.W., Pihalja, M., Weissman, I.L., Morrison, S.J., and Clarke, M.F. (2003). Bmi-1 is required for maintenance of adult self-renewing haematopoietic stem cells. Nature *423*, 302–305.

Prince, M.E., Sivanandan, R., Kaczorowski, A., Wolf, G.T., Kaplan, M.J., Dalerba, P., Weissman, I.L., Clarke, M.F., and Ailles, L.E. (2007). Identification of a subpopulation of cells with cancer stem cell properties in head and neck squamous cell carcinoma. Proc. Natl. Acad. Sci. USA *104*, 973–978.

Rangarajan, A., Hong, S.J., Gifford, A., and Weinberg, R.A. (2004). Species- and cell type-specific requirements for cellular transformation. Cancer Cell *6*, 171–183.

Rodriguez-Viciana, P., Warne, P.H., Khwaja, A., Marte, B.M., Pappin, D., Das, P., Waterfield, M.D., Ridley, A., and Downward, J. (1997). Role of phosphoinositide 3-OH kinase in cell transformation and control of the actin cytoskeleton by Ras. Cell *89*, 457–467.

Sanai, N., Alvarez-Buylla, A., and Berger, M.S. (2005). Neural stem cells and the origin of gliomas. N. Engl. J. Med. *353*, 811–822.

Serrano, M., Lee, H., Chin, L., Cordon-Cardo, C., Beach, D., and DePinho, R.A. (1996). Role of the INK4a locus in tumor suppression and cell mortality. Cell *85*, 27–37.

Singh, S.K., Hawkins, C., Clarke, I.D., Squire, J.A., Bayani, J., Hide, T., Henkelman, R.M., Cusimano, M.D., and Dirks, P.B. (2004). Identification of human brain tumour initiating cells. Nature *432*, 396–401.

Sturn, A., Quackenbush, J., and Trajanoski, Z. (2002). Genesis: Cluster analysis of microarray data. Bioinformatics *18*, 207–208.

Su, I.H., Dobenecker, M.W., Dickinson, E., Oser, M., Basavaraj, A., Marqueron, R., Viale, A., Reinberg, D., Wulfing, C., and Tarakhovsky, A. (2005). Polycomb group protein ezh2 controls actin polymerization and cell signaling. Cell *121*, 425–436.

Tolhuis, B., de Wit, E., Muijrers, I., Teunissen, H., Talhout, W., van Steensel, B., and van Lohuizen, M. (2006). Genome-wide profiling of PRC1 and PRC2 Polycomb chromatin binding in Drosophila melanogaster. Nat. Genet. *38*, 694–699.

Valk-Lingbeek, M.E., Bruggeman, S.W., and van Lohuizen, M. (2004). Stem cells and cancer; the polycomb connection. Cell *118*, 409–418.

Van der Lugt, N.M., Domen, J., Linders, K., van Roon, M., Robanus-Maandag, E., te Riele, H., van der Valk, M., Deschamps, J., Sofroniew, M., and van Lohuizen, M. (1994). Posterior transformation, neurological abnormalities, and severe hematopoietic defects in mice with a targeted deletion of the bmi-1 proto-oncogene. Genes Dev. *8*, 757–769.

van Lohuizen, M., Verbeek, S., Scheijen, B., Wientjens, E., van der Gulden, H., and Berns, A. (1991). Identification of cooperating oncogenes in E mu-myc transgenic mice by provirus tagging. Cell *65*, 737–752.

Wang, L.H. (2004). Molecular signaling regulating anchorage-independent growth of cancer cells. Mt. Sinai J. Med. *71*, 361–367.

Zencak, D., Lingbeek, M., Kostic, C., Tekaya, M., Tanger, E., Hornfeld, D., Jaquet, M., Munier, F.L., Schorderet, D.F., van Lohuizen, M., and Arsenijevic, Y. (2005). Bmi1 loss produces an increase in astroglial cells and a decrease in neural stem cell population and proliferation. J. Neurosci. *25*, 5774–5783.

Zhu, Y., Guignard, F., Zhao, D., Liu, L., Burns, D.K., Mason, R.P., Messing, A., and Parada, L.F. (2005). Early inactivation of p53 tumor suppressor gene cooperating with NF1 loss induces malignant astrocytoma. Cancer Cell *8*, 119–130.

Zhu, Y., and Parada, L.F. (2002). The molecular and genetic basis of neurological tumours. Nat. Rev. Cancer *2*, 616–626.